Graphical Abstract

Advancing Odor Classification Models Enhanced by Scientific Machine Learning and Machanistic Model: Probabilistic Weight Assignment for Odor Intensity Prediction and Uncertainty Analysis for Robust Fragrance Classification

Vinicius V. Santana, Erbet A. Costa, Carine M. Rebello, Ana Mafalda Ribeiro, Chris Rackauckas, Idelfonso B. R. Nogueira

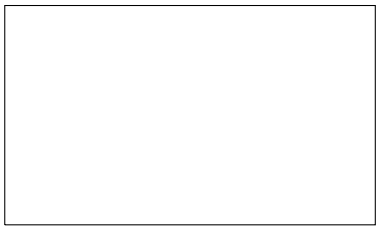

Highlights

Advancing Odor Classification Models Enhanced by Scientific Machine Learning and Machanistic Model: Probabilistic Weight Assignment for Odor Intensity Prediction and Uncertainty Analysis for Robust Fragrance Classification

Vinicius V. Santana, Erbet A. Costa, Carine M. Rebello, Ana Mafalda Ribeiro, Chris Rackauckas, Idelfonso B. R. Nogueira

- Research highlight 1
- Research highlight 2

Advancing Odor Classification Models Enhanced by Scientific Machine Learning and Machanistic Model: Probabilistic Weight Assignment for Odor Intensity Prediction and Uncertainty Analysis for Robust Fragrance Classification

Vinicius V. Santana[a,b,c,*], Erbet A. Costa[c], Carine M. Rebello[c], Ana Mafalda Ribeiro[a,b], Chris Rackauckas[d], Idelfonso B. R. Nogueira[c,*]

[a] *Laboratory of Separation and Reaction Engineering, Catalysis and Materials (LSRE-LCM), Porto, Portugal*
[b] *Associate Laboratory in Chemical Engineering (ALiCE), Porto, Portugal*
[c] *Department of Chemical Engineering, Faculty of Natural Sciences, Norwegian University of Science and Technology, Trondheim, Norway*
[d] *Julia Lab, Computer Science and Artificial Intelligence Laboratory, Massachusetts Institute of Technology, Boston, USA*

Abstract

Lorem ipsum dolor sit amet, consectetur adipiscing elit, sed do eiusmod tempor incididunt ut labore et dolore magna aliqua. Ut enim ad minim veniam, quis nostrud exercitation ullamco laboris nisi ut aliquip ex ea commodo consequat. Duis aute irure dolor in reprehenderit in voluptate velit esse cillum dolore eu fugiat nulla pariatur. Excepteur sint occaecat cupidatat non proident, sunt in culpa qui officia deserunt mollit anim id est laborum.

Keywords: keyword one, keyword two

PACS: 0000, 1111

2000 MSC: 0000, 1111

1. Introduction

Fragrances are deeply embedded in consumer products across the globe, serving as a pivotal element in captivating consumers and fueling purchases. Their core objective is to

*Corresponding author

Email addresses: up201700649@edu.fe.up.pt (Vinicius V. Santana), idelfonso.b.d.r.nogueira@ntnu.no (Idelfonso B. R. Nogueira)

bestow products with a pleasant and harmonious aroma, evoking positive sensations upon interaction. Both a signature of distinction and a source of pleasure, fragrances can elevate a product's desirability and functional appeal to its audience Calkin and Jellinek (1994); Cussler et al. (2010); Teixeira et al. (2011); Butler (2013).

However, crafting a harmonious and pleasant fragrance is complex considering the number of available fragrances (on the order of several thousand) (Teixeira et al., 2011) . The possible combinations of fragrance ingredients for a perfumer are nearly endless – achieving a desired olfactory target involves a long and costly trial-and-error process for testing the perceived odor of hundreds of different samples (Santana et al., 2021). Historically, this intricate process has leaned heavily on the expertise of seasoned perfumers who meticulously adjust ingredient proportions to attain the desired olfactory experience in intensity and quality (Mata et al., 2005; Rodrigues et al., 2021). In the past two decades, the use of Product Engineering in fragrance design has emerged as a valuable tool to integrate scientific knowledge into a traditionally empirical and subjective domain (Mata et al., 2005; Rodrigues et al., 2021; Teixeira et al., 2013a). A notable benefit of this integration is the ability to decrease the number of chemicals in formulations, all while achieving the desired perceptual outcomes.

From the viewpoint of Product Engineering, understanding the perception of a fragrance in a perfume involves a sequence of events, some of which are grounded in well-defined physics and mathematical frameworks: (i) The process commences with a solution of fragrance ingredients and solvents, characterized by specific molar compositions (x_i), which users apply to their skin or clothing. (ii) Upon application, this liquid blend starts evaporating into the ambient atmosphere, resulting in alterations in both nearby gas-phase (yi) and liquid-phase (xi) compositions. (iii) As the evaporation proceeds, the fragrant components spread into the surrounding air. (iv) Ultimately, some fragrance molecules reach the olfactory senses of nearby individuals, conveying distinct intensities and scent characteristics (Teixeira et al., 2011).

In this sense, it is of great interest to establish reliable predictive models that can accurately describe this chain of processes from the release of a scent on a substrate to its

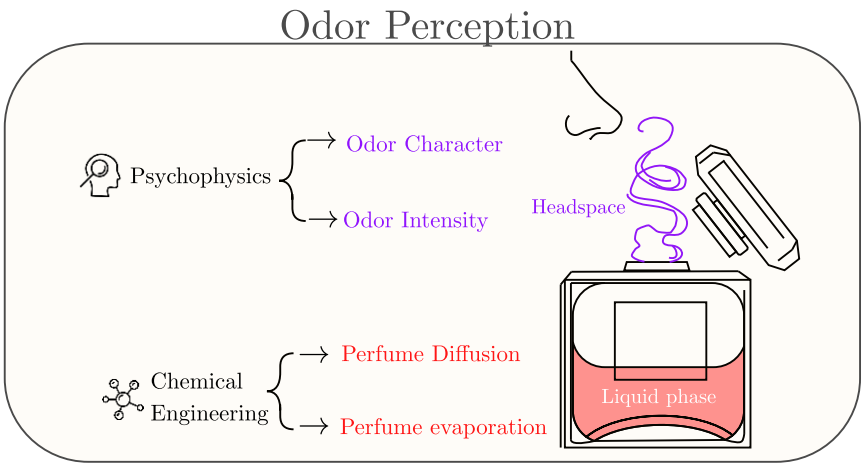

Figure 1: Schematic representation of the steps involved in the odor perception model for fragrance mixtures. Adapted from Teixeira (2011).

reception by the human olfactory system. Once developed and validated, such models offer extensive utility – they can deepen our comprehension of fragrance perception or aid perfumers in the design and formulation processes, for instance.

Over the past decades, advancements in Perfume Engineering have made remarkable strides in integrating well-established physics with the description of scent perception. This integration leans heavily on Chemical Engineering domains, encompassing solution's thermodynamics, transport phenomena, and the psychophysics of human sensory perception. Figure 1 visually represents this intricate chain of processes and highlights the specific scientific disciplines engaged at each juncture. Within this framework, several developments have emerged, such as the Perfumery Ternary Diagrams (PTD) methodology (Mata et al., 2005), the perfume radar (Teixeira et al., 2014), and research on the diffusion and performance of perfume mixtures (Teixeira et al., 2009, 2013b).

From the perspective of the mentioned works, perfumes can be defined as liquid mixtures of odorants dissolved in appropriate solvents, such as a combination of ethanol and water. Chemical Engineering offers models for understanding the transition from liquid to vapor through thermodynamics and the subsequent diffusion of these scents in the air. Furthermore, the concentration of these fragrant molecules can be related to the sensory

experience through models of odor intensity and perception, drawing insights from psychophysics. This provides an appropriate framework for describing and evaluating perfume behavior as demonstrated in Teixeira et al. (2009, 2013b); Zhang et al. (2020).

Although this approach has shown strong predictive capabilities, uncertainties in the model's parameters can significantly influence their predictions and subsequent tasks where the model is applied. The evaporation of ingredients used in the formulation is a pivotal concern for product design. A component's vapor pressure is essential in evaporation rate prediction within this framework. Yet, vapor pressure is often based on limited experiments, introducing a notable degree of uncertainty, particularly for rarer perfume ingredients. Additionally, for more complex mixtures — whether they are non-ideal, azeotropic, or close-boiling — static uncertainties are inherently present in comprehensive thermodynamic models like UNIFAC, UNIQUAC, or NRTL, which are utilized to obtain deviations from ideality through activity coefficients (Ulas and Diwekar, 2004). Therefore, it is important to identify, quantify, and incorporate these uncertainties into the models.

When considering diffusion in model odor perception, the diffusion coefficient can significantly influence predictions about the concentration of fragrance ingredients in the surrounding air. While finding vapor pressure for rare ingredients is challenging, determining the diffusion coefficient in air is even more difficult. Researchers typically rely on predictive correlations derived from noisy experimental data to estimate it. However, as in any estimation process from noisy observations, an irreducible aleatoric uncertainty is associated with the obtained predictive correlation.

From the perspective of perception, that is, how an individual consciously experiences and describes a smell in terms of intensity and its olfactory family for a given concentration of an odorant, a lot of variation is expected among individuals, i.e., different people experience the same smell differently. This variability (uncertainty) poses a significant challenge when using psychophysics to correlate concentrations with scent intensity and associating individual component intensities and olfactory families with the overall perception of a fragrant mixture. In this way, in olfactory perception studies, factors like inherent variability and response bias are inevitable and should be considered (Teixeira et al., 2013a; Chambers

and Wolf, 1996).

Traditionally, the categorization of individual odors or molecules has relied heavily on the expert sensory perception of human evaluators. However, a paradigm shift is occurring, as evidenced by recent works like those of Sanchez-Lengeling et al. (2019) and Keller and Vosshall (2016); Keller et al. (2017). These researchers have adopted machine learning techniques to approach odor classification from a Quantitative-Structure-Odor-Relationship standpoint. They aim to establish correlations between chemical descriptors of individual odorants and their associated olfactory families or nuances.

When it comes to fragrances, which typically comprise 50 to 100 different aromatic components (odorants), the classification challenge grows even more complex. Conventional methods often categorize perfumes into specific classes or families, sometimes further delineating subfamilies or nuances, largely based on empirical assessments. To inject a layer of scientific rigor into fragrance classification, a novel methodology called Perfumery Radar (PR) has been developed, as cited in the work by Teixeira et al. (2014). This approach employs physicochemical models and qualitative descriptors to categorize commercial perfumes systematically.

In Teixeira et al. (2014) methodology, a significant limitation exists in using traditional techniques for weight assignment. This approach risks introducing bias, as it does not consider the probabilistic nature of olfactory classifications. The consequence is a potential failure to capture the full spectrum of odor intensity variations across different molecular components. This rigidity in weight allocation can limit the model's adaptability to new or complex olfactory scenarios, thereby affecting the overall accuracy and reliability of the odor classification model. A further limitation of Teixeira et al. (2014) methodology is the absence of a mechanism for handling uncertainty. These uncertainties can manifest from the mechanistic models describing perfume diffusion and the variable classifications within olfactory families for individual odorants. Additionally, it is essential to identify, quantify (when feasible), and integrate these uncertainties into the predictive modeling tools used for designing fragrance mixtures.

Building upon Teixeira et al. (2014), our methodology introduces two key advancements:

weight assignment using scent classifier output probabilities and an integrated uncertainty analysis framework. The former enhances the model's adaptability in diverse olfactory landscapes, while the latter fortifies its robustness and generalizability, especially in real-world settings with data imperfections. Uncertainties are quantified via probability statements and density functions, which are derived from prediction residuals for least squares estimated parameters.

These quantified uncertainties are then propagated through the perfume diffusion model using sampling methods, allowing us to assign probabilities to dependent variables, such as the likelihood of evoking a specific olfactory response. This holistic approach not only addresses the limitations of the original work but also paves the way for more robust and reliable fragrance design.

2. Methodology

This section is divided into three parts. The first and second parts detail the perfume diffusion and odor perception models. The third part identifies the source of uncertainties and proposes ways to quantify them.

2.1. Perfume diffusion model

This study employs as a base the perfume diffusion model previously proposed and validated by Teixeira et al. (2009, 2013b). The proposed model focuses on the amount of liquid perfume typically released with a single spray. The model aims to simulate the evaporation process observed when a perfume bottle's diffuser is pressed. To validate the methodology proposed here, a mixture of limonene, geraniol, vanillin, and ethanol, also investigated in Teixeira et al. (2010), was used as a case study. The initial composition of the components is 0.12, 0.12, 0.06, 0.7, respectively.

The model aims to describe the evaporation of a small amount of liquid perfume, which rises through the air above it (headspace) in the axial direction z dominantly by diffusion where interactions between the scent in the gas phase and surrounding air molecules are negligible, implying an ideal gas phase. It is assumed that the ambient air does not mix

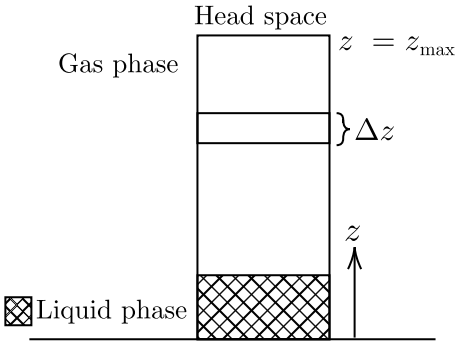

Figure 2: Scheme of the simulated liquid and gas phases of the perfume system. Adapted from Teixeira et al. (2009)

with the liquid and that mass transfer resistance in the liquid can be neglected due to the small quantity of liquid. Figure 2 illustrates the modeled process.

Over time, as evaporation proceeds, the volume and composition of the fragranced mixture change. The liquid phase number of moles is denoted by n_i, while the concentration of each component in the air is represented by c_i. Additionally, it is assumed that the evaporation happens at constant pressure (P) and temperature (T).

Considering the above conditions, the time-dependent mass balance in the gas phase can be expressed by the following partial differential equation (PDE):

$$\frac{\partial y_i}{\partial t} = D_{i,air}\frac{\partial^2 y_i}{\partial z^2} \tag{1}$$

Here, y_i represents the mole fraction of component i in the gas phase, linked to the gas-phase concentration as $C_{i,g} = y_i C_T$. In this relation, C_T is the total concentration in the gas phase, defined by both pressure and temperature. The variable t stands for time, z the direction perpendicular to the liquid-gas interface, while $D_{i,air}$ indicates the diffusivity of component i in the air. $D_{i,air}$ was estimated from Fuller et al. (1966) correlation and given as:

$$D_{i,air} = \frac{1 \times 10^{-8} T^{1.75} \left(\frac{1}{M_i} + \frac{1}{M_{air}}\right)^{1/2}}{P[(\sum_A v_i^{1/3} + 20.1^{1/3})]} \tag{2}$$

v_i is the Diffusion Volume based on the group contribution method and tabulated in the work, T is the temperature in Kelvin, P is the pressure in atm, M_i is the molecular weight in g/mol.

The PDE requires two boundary conditions at the extrema of the z domain. They can be written as:

$$t > 0, z = 0 : y_i(t, z) = \frac{\gamma_i(x_i(t), T) x_i(t) P_i^{\text{Sat}}(T)}{P}; x_i(t) = \frac{n_i(t)}{\sum_{i=1}^{N} n_i(t)} \tag{3}$$

$$t > 0, z = z_{\max} : y_i(t, z) = 0 \tag{4}$$

As seen from Equation 3, the vapor-liquid equilibrium is predicted using Raoult's law, and the liquid-phase non-ideality accounted by the activity coefficients (γ_i) calculated using the UNIFAC Dortmund group-contribution method (Poling et al., 2001; Gmehling, 2003; Gmehling et al., 2002). y_i and x_i are the mole fractions of the i$^{\text{th}}$ component in the gas and liquid phase, respectively. N is the number of components, $P_i^{\text{Sat}}(T)$ is the saturation pressure at temperature T.

The liquid-phase mass balance can be written considering the mass transfer of the components across the interface. This is represented by the subsequent ordinary differential equation (ODE):

$$\frac{dn_i}{dt} = D_{i,air} A_{l,g} C_T \frac{\partial y_i(z = 0, t)}{\partial z} \tag{5}$$

in which n_i is the number of moles of component i in the liquid phase, $A_{l,g}$ is the area of the liquid–gas interface.

2.1.1. Simulation - Numerical solution and software implementation

The perfume diffusion simulator was implemented in the open-source Julia Programming Language (Bezanson et al., 2012). The code is publicly available in the GitHub repository described in the Code Availability section.

To numerically solve the PDE, we employed the method of lines. The axial coordinate z was discretized into an evenly-spaced grid with 40 nodes. The second-order derivative in

Equation 1 was approximated with a centered finite difference scheme, i.e.:

$$\frac{\partial^2 y_i}{\partial z^2} \sim \frac{y_{n+1} - 2y_n + y_{n-1}}{h^2} \tag{6}$$

where n is the grid node index, i.e., $n \in \{1, 2, ..., 40\}$, and h is the distance between two nodes in the grid.

The derivative at $z = 0$ in Equation 5 was approximated using a 3-point forward difference for improved accuracy of flux calculation at the boundary:

$$\frac{\partial y_i(z = 0, t)}{\partial z} \sim \frac{-y_3 + 4y_2 - 3y_1}{2h} \tag{7}$$

The assignment of UNIFAC Dortmund groups for each component in the chosen mixture (limonene, geraniol, vanillin, ethanol) was automated using the GCIdentifier.jl library using the SMILES representations as inputs. Subsequently, activity coefficients were computed using the Clapeyron.jl (Walker et al., 2022) library in the Julia programming environment.

The resulting ordinary differential equation (ODE) was integrated using a fixed-leading coefficient adaptive-order adaptive-time BDF method (FBDF) for stiff ODEs available in DifferentialEquations.jl (Rackauckas and Nie, 2017).

In Fuller et al. (1966) correlation, the groups required for calculating diffusion volumes were also automated using RDKit python API.

2.2. Odor intensity perception model

Of the various models, the Odor Value (OV) is a simple yet intuitive, dimensionless variable that estimates the scent intensity of fragrant molecules. The OV is determined by dividing the concentration of an odorant species i in the gas phase, denoted as $C_{i,g}$, by its odor threshold concentration, Thr_i.

In odor science literature, four principal types of odor thresholds are commonly discussed:

- Detection Threshold (Absolute Odor Threshold): The minimum concentration at which an odor becomes detectable.
- Recognition Threshold: The concentration at which the odor is detectable and identifiable.

- Terminal Threshold: The point at which the odor becomes pungent or irritating.
- Difference Threshold: A comparative or relative odor evaluation, quantifying the minimum change in stimulus—such as gas concentration—required to produce a noticeable difference in perception.

Experimentally, the Difference Threshold is often determined by comparing a standard stimulus to a variable one, measured on a metric scale (Teixeira et al., 2013a). Despite these numbers' differences, detection thresholds are often reported and used in perfume engineering. In this way, it was also employed in this work.

The OV considering the detection threshold of a component i can be written as:

$$OV_i = \frac{C_{i,g}}{Thr_i} \tag{8}$$

When several components are present in the air, the perception of that mixture will be affected by all components. The perception of a mixture of odorants is a complex process not understood thoroughly (Teixeira et al., 2011; Gilbert, 2008). Several models have been proposed to explain the perception of odorants in mixtures, although no consensus was reached about the best one (Laffort and Dravnieks, 1982; Cain et al., 1995; Olsson, 1998). The stronger component model is the simplest and most often used in Product Engineering of fragrant mixtures. It states that the one with the highest odor intensity is the most strongly perceived in a mixture of odorants. It means that the odor with the highest intensity determines the odor intensity of the mixture:

$$OV_{mix} = \max\{OV_1, OV_2, ..., OV_N\} \tag{9}$$

The odor intensity model can be linked with the perfume diffusion model by substituting its numerical solution in the odor value expression. In this way, if $C_{i,g}$ is a variable distributed in (t, z), one can know the corresponding odor value in time and space.

2.3. Odor classification

Building on the work in Teixeira et al. (2014), we also classify scents by combining the olfactory families and predicted intensities of individual odorants. However, we improve upon this by using a probabilistic approach to construct the radar chart initially proposed in Teixeira et al. (2014). Unlike the original study, which used arbitrary weights for olfactory families, our method uses a classifier to calculate the probability for each family of odorants.

The classifier comes from the methodology, the Principal Odor Map (POM), outlined in the study by Lee et al. (2023). Barsainyan (2023) reproduced the methodology and made the model implementation publicly available. A comprehensive dataset was curated by extracting the CAS number of odorants and their corresponding smell semantic descriptors. This curated data set has been organized into a well-structured data frame with records and made publicly accessible via a GitHub repository.

The POM approach employed the message-passing neural network classifier. The molecules were encoded into adjacency and feature matrices. The feature matrix includes binary features regarding each atom's atomic type, bonding properties (orbitals hybridization), and the presence of a chirality center. The target variable was a 138-dimensional binary vector, indicating an odorant's membership in various olfactory families.

2.4. Uncertainty quantification and propagation

The predictive perfume diffusion and odor intensity models contain parameters/variables $(T, P, D_{i,air}(T,P), P^{Sat}(T), \gamma(x,T), Thr_i, A_{l,g})$ that must be known to be used for predictions. These quantities contain uncertainty as they are estimated from direct or indirect noisy observations. This section describes the methodology used to quantify uncertainties using probability theory and the method to propagate them through the simulator.

While this study addresses the uncertainties in $D_{i,air}(T,P)$, $P^{Sat}(T)$, and Thr_i, it should be noted that temperature and pressure (T,P) can also fluctuate during experimentation, affecting the results. However, these factors are not considered the most critical variables for the scope of this work. Another important parameter is the area at the gas-liquid interface $A_{l,g}$, commonly set at 0.071 m^2 (Teixeira et al., 2013a). However, no rational basis exists

for this specific value in the literature. Consequently, this study does not account for the uncertainty associated with this particular parameter. Finally, the uncertainty in the activity coefficient $\gamma(x, T)$ significantly influences predictions, as quantified in distillation processes in (Ulas and Diwekar, 2004). Unfortunately, an accurate assessment of the uncertainty of this variable requires multiple measurements of liquid-vapor equilibrium, which are unavailable for the case study mixture explored here, consisting of limonene, geraniol, vanillin, and ethanol.

2.4.1. Quantifying uncertainties from Least Squares Estimation (LSE) of parametrized models: Vapor Pressure and diffusion coefficient

In the literature, vapor pressure is commonly obtained from the Antoine equation ($\log P_{sat} = A - \frac{B}{T_{sat}+C}$). It relates the saturation temperature T_{sat} with the saturation pressure P_{sat} valid in a limited range of temperatures and pressures. To estimate the parameters, a finite number of P, T noisy data is collected, forming a data set $\mathcal{D}_{P,T} = \{(P_{sat,1}, T_{sat,1}), ..., (P_{sat,N}, T_{sat,N})\}$, where N is the number of observations, and used in an estimation problem. In this context, the target variable is usually either the temperature or the logarithm of the pressure, which turns the other variable into a predictor.

For diffusion coefficients, the correlation proposed by Fuller et al. (1966) has been utilized in perfume engineering, specifically within the perfume diffusion model as cited in studies by Teixeira et al. (2013b, 2009). The authors assert that this model offers satisfactory accuracy when applied to volatile compounds diffusing through air. The correlation has grounds in the hard-sphere model from the Chapman-Enskog equation (Chapman and Cowling, 1990). However, Fuller et al. (1966) proposed an improved form of the equation that contains parameters to be identified from experimental data, i.e., from a data set $\mathcal{D}_{D_{i,j},P,T} = \{(D_{1,j}, P_1, T_1), (D_{2,j}, P_2, T_2), ..., (D_{N,j}, P_N, T_N))\}$, where $D_{i,j}$ is given by:

$$D_{i,air} = \frac{CT^b \left(\frac{1}{M_i} + \frac{1}{M_j}\right)^{1/2}}{P[(\sum_A v_i^{\alpha_1} + \sum_A v_j^{\alpha_2})]} \tag{10}$$

v_i is the diffusion volume based on the group contribution method, C is an arbitrary constant, b is the exponent dependency of temperature, and α_1, α_2 are the diffusion volumes'

exponents. All parameters were identified by solving an estimation problem. In such work, C, b, α_1, α_2 were found to be $1 \times 10^{-8}, 1.75, 1/3, 1/3$, respectively for T in K, P in atm, M_i in g/mol, $D_{i,j}$ in cm^2/s. The Diffusion Volumes can be found in Fuller et al. (1966) work.

There are two predominant methods to formulate and solve the estimation problem: the frequentist and Bayesian approaches. The frequentist method, owing to its simplicity, is more widely used. This approach can be derived using the maximum likelihood principle, resulting in the Least Squares Estimation (LSE).

To associate the LSE with a probability density function post-estimation (point predictive distribution), it is essential to derive it from the maximum likelihood principle. The initial step involves assigning a probability density function (pdf) or likelihood function to the data generation process. In LSE, the Normal distribution ($\mathcal{N}$) with a mean equal to the predictive model ($\phi(x, W)$) with predictors x, parameters W and unknown variance σ^2 is used:

$$y_i \sim \mathcal{N}\left(y_i | \phi(x_i, W), \sigma^2\right) \tag{11}$$

In this work, $\phi(x, W)$ can be either the Antoine equation if the prediction is for vapor pressure or Fuller et al. (1966) correlation (Equation 10) if the prediction is for diffusion coefficient in air.

From the pdf of a single observation and assuming that all observations are independent and identically distributed (iid), we can write:

$$y_{1:N} \sim \prod_{i=1}^{N} \mathcal{N}\left(y_i | \phi(x_i, W), \sigma^2\right) \tag{12}$$

$$p\left(y_{1:N} | \phi(x_{1:N}, W), \sigma^2\right) = (2\pi\sigma^2)^{-\frac{N}{2}} \exp\left\{\frac{-1}{2\sigma^2} \sum_{i=1}^{N} \left(y_i - \phi(x_i, W)\right)\right\} \tag{13}$$

To determine all the parameters, we employ the maximum likelihood function. This encompasses parameters from the Antoine or diffusivity coefficient equations and the measurement variance, denoted as σ^2. Given that the values of the likelihood function can be close to zero, it is often more practical to minimize the negative logarithm of the likelihood. By doing so, we derive:

$$\min_{W,\sigma^2} \mathcal{J} = -\log\left\{p\left(y_{1:N}|\phi(x_{1:N},W),\sigma^2\right)\right\} = \left\{\frac{N}{2}\log(2\pi) + \frac{N}{2}\log(\sigma^2) + \frac{1}{2\sigma^2}\left|\left|\left(y_{1:N} - \phi(x_{1:N},W)\right)\right|\right|^2\right\} \tag{14}$$

Using deterministic optimization methods, taking the derivative of $\mathcal{J}$ with respect to W and setting it to zero, W optimal can be estimated. Once W has been estimated, σ^2 can be estimated by setting $\frac{d\mathcal{J}}{d\sigma^2} = 0$. This yields an analytical representation for σ^2 as:

$$\sigma^2 = \frac{1}{N}\sum_{i=1}^{N}\left(y_i - \phi(x_i,W)\right)^2 \tag{15}$$

Though this formula is commonly termed the Mean Squared Error (MSE), from a statistical lens, it corresponds to the estimation of the variance of the likelihood function.

Finally, we can incorporate this measurement uncertainty when making predictions. This is done through the point predictive distribution, which is Normal:

$$p(y|\phi(x,W),\sigma^2) = \mathcal{N}(\phi(x,W),\sigma^2) \tag{16}$$

After estimation, however, verifying if the residuals follow the Normal distribution, as assumed in likelihood, and if the variance is constant is important. The normality of residuals can be verified by the goodness-of-fit Kolmogorov–Smirnov test (Massey, 1951). The homogeneity of the variance can be verified by visual inspection with parity plots or using adequate testing statistics, e.g., Levene's test.

2.4.2. Quantifying uncertainties of odor threshold

Various techniques and equipment may be employed for the calculation of odor thresholds. An average odor threshold value can be ascertained by examining the distribution of relative sensitivity to a specific chemical odorant across a large population. It is important to recognize that although this final result may appear as a single threshold value or an estimated range of values with accompanying confidence limits, it is based on a substantial amount of underlying experimental tests. Inherent variability and response bias are unavoidable factors in olfactory perception studies. Even within the same panel, individual

responses can vary significantly—ranging from a two-fold to a four-fold difference in the same experiment (Chambers and Wolf, 1996). Interpersonal variability can be even more pronounced, with differences sometimes escalating to as much as three orders of magnitude (Teixeira et al., 2013a).

Individual and interpersonal variability must be considered to quantify the uncertainty linked with odor detection thresholds comprehensively. A major obstacle in achieving this comprehensive understanding is the absence of standardized methods for reporting such metrics. While some studies report confidence intervals, others only offer a single threshold value, as is often seen in compilations of odor thresholds (van Gemert, 2011). We suggest employing a weighted sum of probability density functions to address these varying conditions.

For cases where an interval is reported, a uniform probability density function is assigned to that range. When only a single value is reported, a Dirac delta function is the probability density function for that specific number. If a combination of these two scenarios exists for a given component, we construct a weighted sum of probability density functions, assigning equal weights to each. This is based on the assumption that opting for a conservative distribution ensures robustness in the model. This approach is particularly relevant for input variables whose underlying distribution is unknown or insufficiently characterized. This assumption maximizes our findings' reliability in cases where the data is limited or ambiguous.

In this study, diffusion, vapor pressure, and threshold concentration uncertainties are explicitly characterized using conservative statistical methods. For other significant variables — namely surface area and activity coefficient—either data are insufficient, or no established methodology exists for uncertainty quantification. While the present work does not encompass all sources of uncertainty, it is an initial effort to integrate uncertainty related to threshold values within the perfume engineering framework, thereby providing a basis for future advancements in robustness and accuracy.

2.4.3. Propagating uncertainty through the perfume diffusion simulator

In uncertainty quantification using probability theory, sampling methods are often utilized to propagate uncertainty through a simulator, yielding samples of dependent variables. In this study, our main focus is to obtain samples in the odor intensity in time and space for each component in the mixture, namely limonene, geraniol, vanillin, and ethanol. To accomplish this, we sample from the probability density functions of all uncertain parameters and run simulations of the perfume diffusion model for each set of samples. While it is possible to calculate statistical metrics such as expectation and variance related to odor intensity without propagating uncertainty, as suggested by the Koopman operator discussion in SciMLExpectations.jl, the present work opted to estimate these metrics using output samples.

Various sampling methods are available for this type of analysis, ranging from the straightforward "crude" Monte Carlo method, which utilizes a pseudo-random generator to approximate a uniform distribution, to more advanced techniques specifically designed for multivariate distribution sampling. Such specialized methods include Latin Hypercube Sampling (Hardin and Sloane, 1993) and Sobol sequences (Sobol', 1967). It is worth noting that, theoretically, quasi-Monte Carlo methods such as Sobol sequences are low-discrepancy and therefore converge as integral approximations at a rate of $O(n)$, in contrast to the $O(\sqrt{n})$ convergence rate of a naive Monte Carlo method. This theoretical framework highlights the potential differences in convergence speed. In the present work, the convergence rates for calculating expectation, variance, and percentiles are compared between the crude Monte Carlo and Sobol sampling methods.

The built pdf samples were obtained using Distributions.jl (Lin et al., 2019; Besançon et al., 2021) along with MonteCarloMeasurements.jl (Bagge Carlson, 2020) for crude Monte Carlo and QuasiMonteCarlo.jl for Sobol sampling.

2.5. Integration of models for robust fragrance odor classification

While we have based our approach on the work by Teixeira et al. (2014) for integrating the perfume diffusion model with odor classification, our method introduces several

enhancements. As a first contribution, we integrated a unique methodology to cope with uncertain outcomes within the odor classification model, something not present in the original work. For a more visual understanding of this work's contribution, the methodology is schematically and visually depicted in Figure 3.

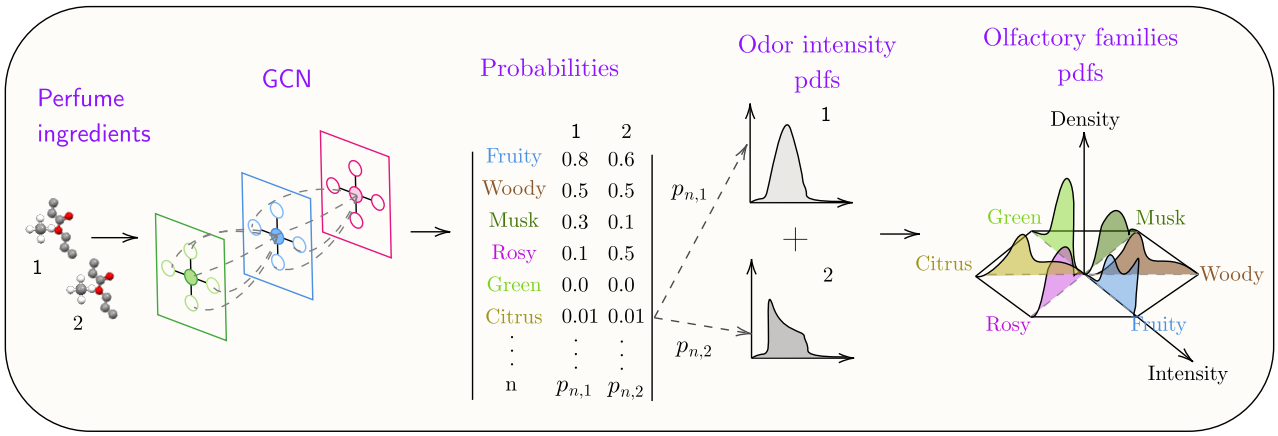

Figure 3: Diagram for the methodology of robust fragrance classification (olfactory families are generic).

3. Results

Furthermore, a significant feature of our method lies in its utilization of the classifier's output probabilities. Instead of traditionally assigning weights, we use these probabilities as an unbiased technique to allocate weights to each molecule's odor intensity probability distribution function.

In the process, the probabilities of different olfactory families, determined by the GCN, serve as these weights. When multiplied with the odor intensity trajectories of each component, each radar segment corresponding to an olfactory family becomes a weighted combination of these trajectories.

3.1. Quantifying uncertainties of diffusion coefficient and vapor pressure

Using the methodology outlined in Section 2.4.1, a point predictive distribution of the diffusion coefficient based on data from Fuller et al. (1966) was identified. This data comprises the diffusion of 40 compounds in the air and provides predictions and their absolute deviations. A histogram of the error distribution was plotted to evaluate its similarity to a potential Normal likelihood function (Figure 4). To confirm the hypothesis of a Normal likelihood, the Massey (1951) goodness-of-fit Kolmogorov-Smirnov (K-S) test was applied, where the null hypothesis postulates that the sample does not result from a Normal distribution with zero mean and standard deviation equal to 8.4297×10^{-7} calculated using Equation 15.

The K-S test provided a p-value of 0.6977, suggesting insufficient evidence to reject the null hypothesis.

This work assumes that for all the molecules in the fragrant mixture (limonene, geraniol, vanillin, ethanol), the point-predictive distribution of the air diffusion coefficient is given by a Normal distribution with mean equal to correlation 10 and standard deviation 8.4297988×10^{-7}.

It was assumed that the residuals for the saturation temperature follow a normal distribution. To test this hypothesis, vapor pressure data for the solvent, ethanol, was sourced from the Dortmund Data Bank (GmbH, 2023). This data was then compared with the

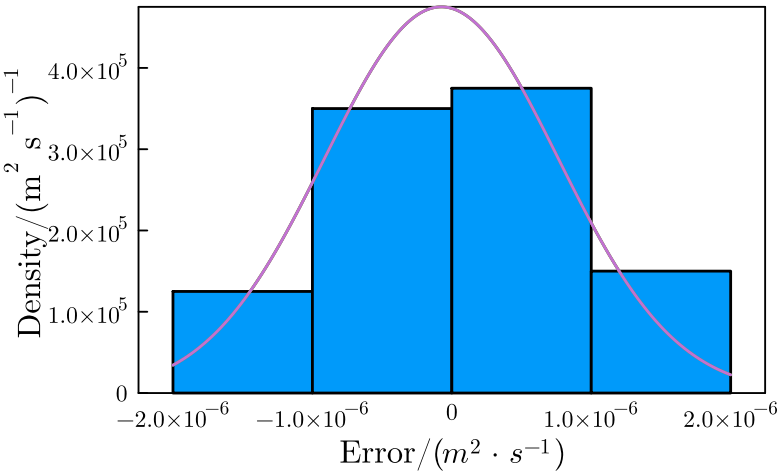

Figure 4: Histogram of the error of diffusion coefficients in air.

Antoine Equation, represented as $T_{\text{sat}} = \frac{B}{A - \log_{10} P + C}$, with $A = 7.239$, $B = 1582.195$, and $C = -48.855$. The data set encompasses 68 liquid-vapor equilibrium records for ethanol, ranging in temperature from 290.25 K to 351.70 K. A histogram of the saturation temperature error distribution was plotted to evaluate its similarity to a potential Normal likelihood function (Figure 5).

The K-S test was employed to validate the assumption of a normal distribution. The null hypothesis of this test posits that the sample is drawn from a normal distribution with a mean of zero and a standard deviation of approximately 0.1468. The K-S test provided a p-value of 0.1285, suggesting insufficient evidence to reject the null hypothesis. This result indicates that the residuals of the saturation temperature of ethanol appear to follow a normal distribution. Notably, the saturation pressure is the primary variable of interest in the perfume diffusion model. When isolating P in the Antoine formula, the resulting probability density function (pdf) for saturation pressure appears to follow a lognormal distribution. This is consistent with the lower boundary of this variable, which is greater than zero.

An alternative approach was implemented to address the lack of readily available experimental vapor-liquid equilibrium data for the remaining components of the fragrant mixture (limonene, geraniol, and vanillin). Given the challenges in sourcing tabulated data, we em-

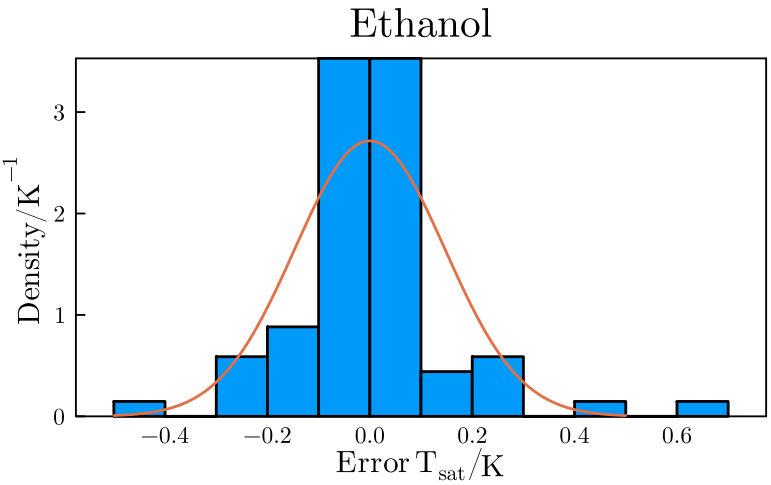

Figure 5: Histogram of the error of ethanol's saturation temperature

ployed a different methodology. Instead of evaluating the saturation temperature residual distribution, we used an estimate of the saturation temperature standard deviation. This estimate was obtained from the reported root mean squared errors (RMSEs) in Stephenson and Malanowski (1987).

It is worth noting that the handbook referenced also contains standard deviation values for ethanol, which exhibited values closely aligned with those we obtained through our estimation process (reported 0.02 - 0.1, this work 0.1468). This consistency underscores the reliability of our approach, affirming that it yields a robust approximation for this variable. The Antoine parameters chosen for limonene, geraniol, and vanillin were tailored for predictions at the simulated temperature of 298.15 K. Table 1 provides the Antoine parameters and estimated standard deviation (σ) of saturation temperature for each component.

Substance	A	B	C	σ (K)
Limonene	6.81591	2075.62	-16.65	1.0
Geraniol	8.64144	3287.427	0.0	5.0
Vanillin	10.9356	4535.023	0.0	5.0

Table 1: Antoine parameters and standard deviations for selected substances.

3.2. Quantifying uncertainties of odor threshold

Following the approach detailed in Section 2.4.2, we model the odor threshold uncertainty using a mix of uniform and delta distributions. The van Gemert (2011) reported odor thresholds exhibit significant variability in the mixture examined. Specifically, limonene has values of 0.21 and 1.7 mg/m^3. This near eightfold increase in threshold values indicates a considerable range in the odor sensitivity for this compound. Geraniol shows an even greater contrast, with values listed as 7.1×10^{-4} and 0.6 mg/m^3, suggesting an approximate 850 times difference between the lower and upper threshold. Vanillin's range, from 7×10^{-5} to 0.005 mg/m^3 (modeled as Uniform distribution), highlights a 70 times difference, indicating potentially varying perceived intensities in different contexts. Notably, ethanol presents the most diverse range. Its 11 values span from 0.17 mg/m^3 to 1350.0 mg/m^3. This vast range, nearly 8000 times from the lowest to the highest value, underscores the potential variability in its odor perception, possibly due to multiple sources of data and different experimental conditions.

The observed variability in odor thresholds holds significant implications for the model-based design of fragranced mixtures. Different selections of thresholds can lead to vastly different mixture designs. When this variability is coupled with the uncertainties inherent in the perfume diffusion model, several orders of magnitude can diverge the resulting predictions.

3.3. Uncertainty propagation

To propagate the uncertainty of the parameters through the perfume diffusion model, 60,000 samples were drawn from each presented probability density function using both "crude" Monte Carlo and Sobol sequences as described in the methodology, except for those that are Dirac mixtures—specifically, the odor thresholds for limonene, geraniol, and ethanol. To estimate statistics of the odor values of these components, samples from the concentration are apportioned among each discrete possible value that can be assumed. For example, given that the limonene threshold can be either 0.21 or 1.7, the 60,000 trajectories are effectively doubled to 120,000 by dividing each trajectory by each threshold value.

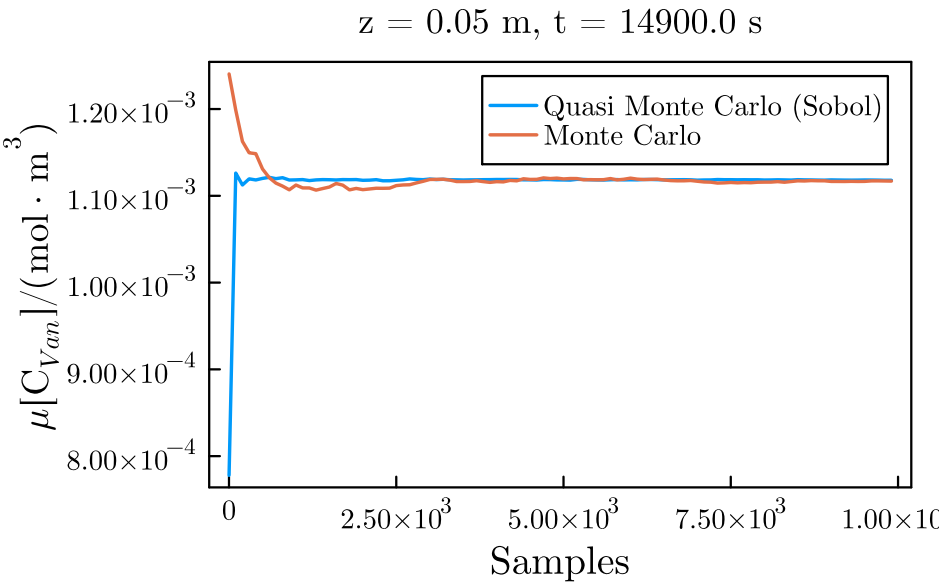

Figure 6: Evolution of the expected value of geraniol concentration close to the perfume source and 14900s after the release

The quantity of samples was predetermined, taking into account the runtime of the perfume diffusion model. Nevertheless, to visually assess the appropriate cutoff value for the number of samples, a convergence verification of summary statistics (mean) was executed for both sampling methods. Upon reaching this number, it is reasonable to infer that the sampling statistics exhibit negligible variation.

To observe the convergence of the mean gas-phase concentration, samples taken near the releasing source and after an extended period were employed as reference points for geraniol, given that variations under these conditions are more pronounced, as depicted in Figure A.14. Figure 6 illustrates that Sobol Sampling demonstrates earlier convergence than Crude Monte Carlo, in line with expectations.

To first understand how the vapor pressure and diffusivity uncertainties affect the predictions, the mean gas phase concentration and 99% credible interval (spanning the 5th to 99.5th percentiles) at a 100cm distance from the liquid-gas interface is displayed in Figure 7 for crude Monte Carlo samples. It can be seen that predictions can differ by orders of magnitude with amplifying intervals as time evolves. The least pronounced amplitude of

the credible interval is related to ethanol, as expected due to its lower variance in the vapor pressure point predictive distribution. Similar figures were plotted to illustrate the same conclusions at different positions from the liquid source and are displayed in the Appendix A.

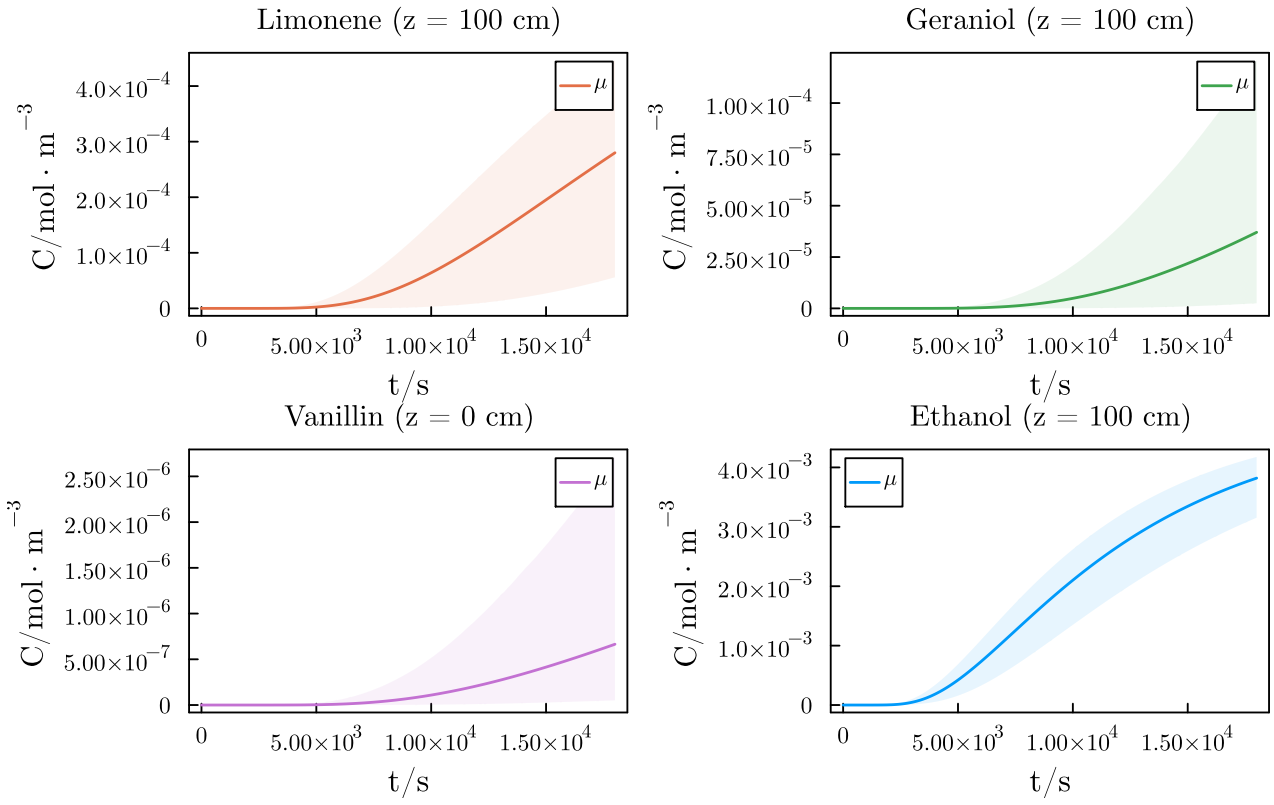

Figure 7: Mean gas phase concentrations and 99% credible intervals for all components at z = 100cm

3.4. Integration of models for robust fragrance classification

After analyzing the uncertainties in the mechanistic model—specifically, the effects of vapor pressure and diffusivity uncertainties on the gas phase concentration of odorants—we can apply our proposed framework (shown in Figure 3). This framework integrates concentration trajectories, the psychophysics model's uncertainty, and the output probabilities from the odor classifier into a unified structure.

To accomplish the integration, the membership probabilities of 139 olfactory families were estimated for every molecule in the studied fragrance mixture (limonene, geraniol,

vanillin, and ethanol). Only the families with probabilities higher than 0.55 were kept as they were highly certain to be present. Figure 8 displays each molecule's corresponding values.

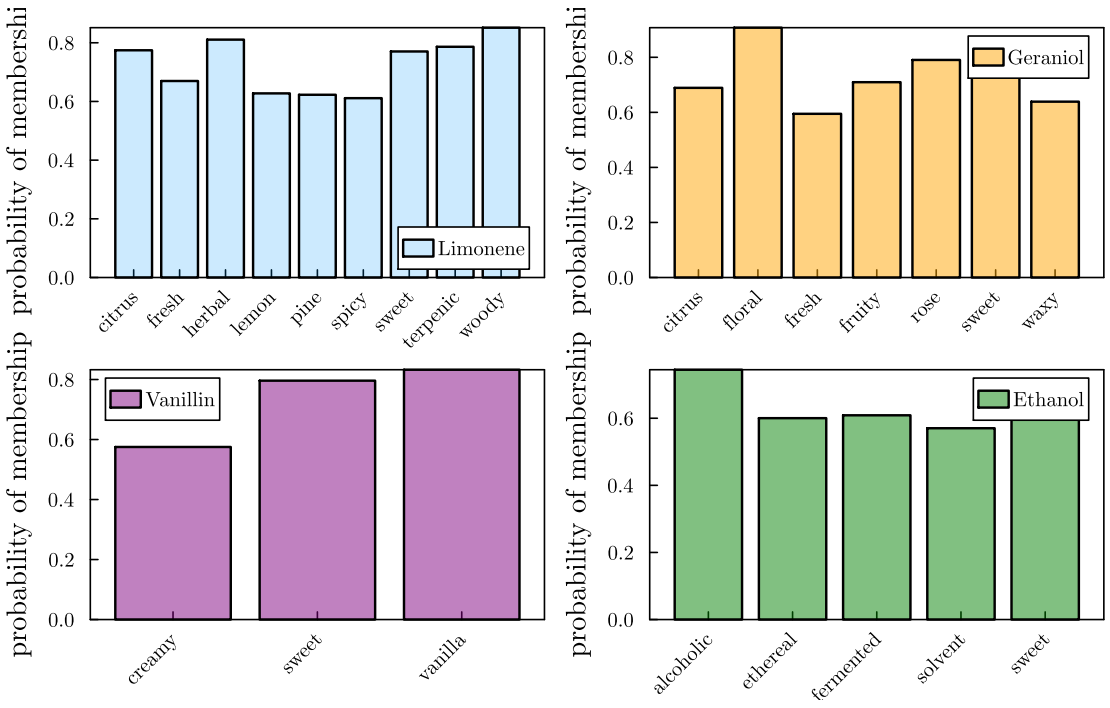

Figure 8: Estimated probabilities of membership for each ingredient in the fragrant mixture

These probabilities acted as weight factors to determine each family's composite odor intensity field samples $\psi_f(z,t)$. For the citrus family, as an illustration, the field is computed by taking the product of the membership probability of limonene to the citrus category with the odor intensity field samples of limonene. Subsequently, the result from the product of geraniol's citrus membership probability and its odor intensity field samples is added to this value.

The probability densities associated with each family allow for visualizing the odor intensity field samples. However, with 19 families, it becomes challenging to represent them clearly in a single graph, especially because each point in the z, t grid is a set of 19 samples with thousands of points. As a representation, Figure 9 displays a subset, illustrating the estimated densities for 6 odor intensities using kernel density estimation at time t = 4 s at

a distance of 0.05 m from the releasing source. The intention is to characterize the odor shortly after the release and near the source. It can be seen that the sweet intensity is dominant over the remaining 5 ones displayed.

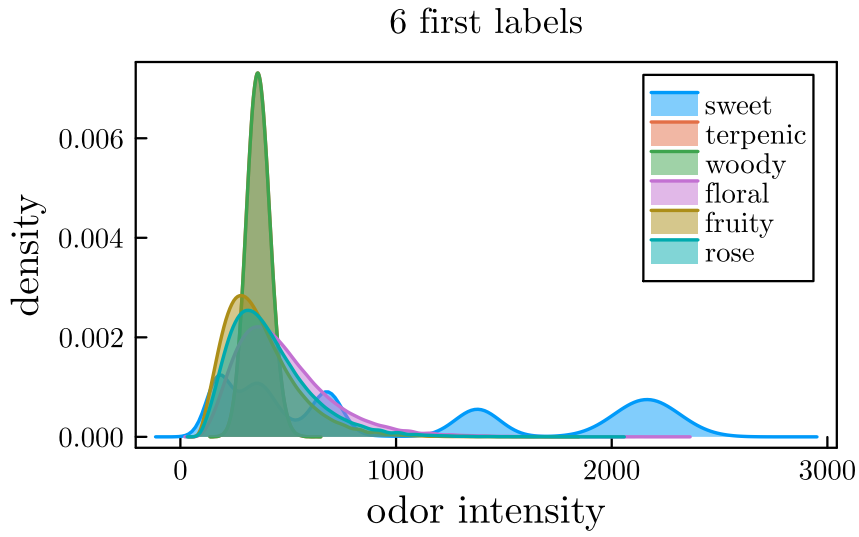

Figure 9: Probability density estimation of 6 olfactory families intensities at z = 0.05 m, t = 4 s

To better understand the dominant families, we averaged the intensity distributions for each family and displayed them in increasing order of intensity in Figure 10. It can be seen that the intensities associated with ethanol are the ones with the highest intensities, and "alcoholic" is the olfactory family with the highest intensity, followed by fermented and ethereal. Creamy and vanilla are the ones with the lowest values.

In addition to determining the intensities of each olfactory family, we can also evaluate which family is most dominant using a probabilistic approach. Specifically, we can estimate the probability of an olfactory family being dominant by counting the relative frequency with which it exhibits the highest intensity. A radar chart can represent the top 7 probabilities (Figure 11). The probabilities estimation follows the same order as the intensity rank, with the highest being alcoholic dominating the scent character in about 25% of the samples, followed by ethereal and fermented in 16% of the samples.

A similar analysis can be performed to understand the perfume character after a few minutes of the release and at a higher distance from the source. In this case, the same

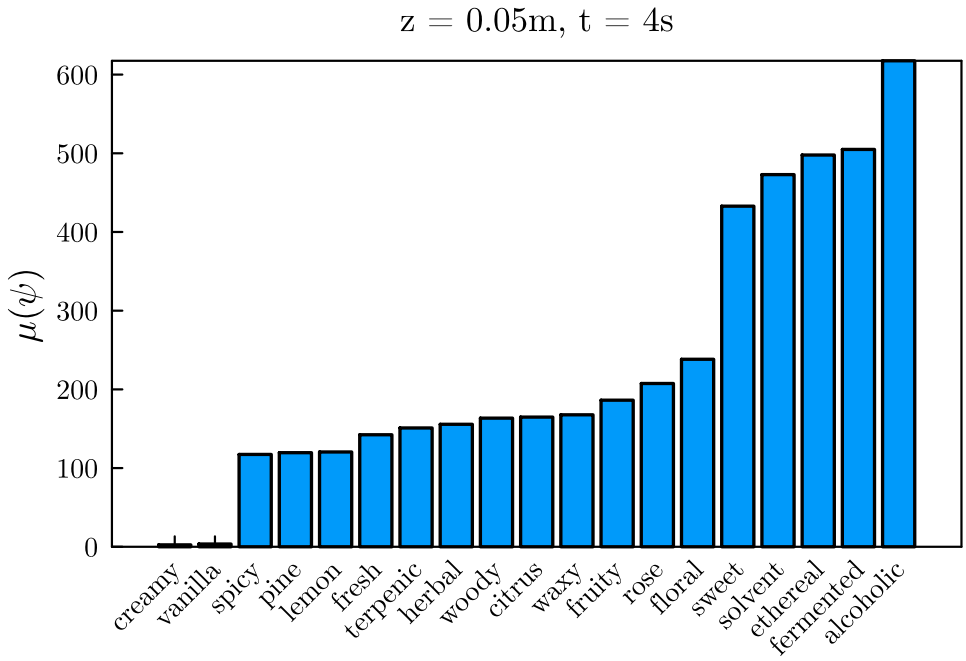

Figure 10: Average intensity distributions for each odor family, presented in ascending order of intensity - z = 0.05 m, t = 4 s.

analysis was conducted at 20 cm and 600 s after the release. Figure 12 shows the averaged intensities of each family. It can be seen that the intensities are considerably smaller than near the source and that the highest average intensity is the "woody" note, followed by "herbal" and "terpenic" (all similarly intense). The estimation of the dominance probability was also estimated and displayed in Figure 13. The probability estimates also follow the same order as the intensity, with about 30% of the samples being dominated by the "woody" note.

By employing these probabilistic statements, this work can be expanded towards robust optimization to maximize the likelihood of attaining a specific olfactory experience, given the known constraints and uncertainties in the model variables.

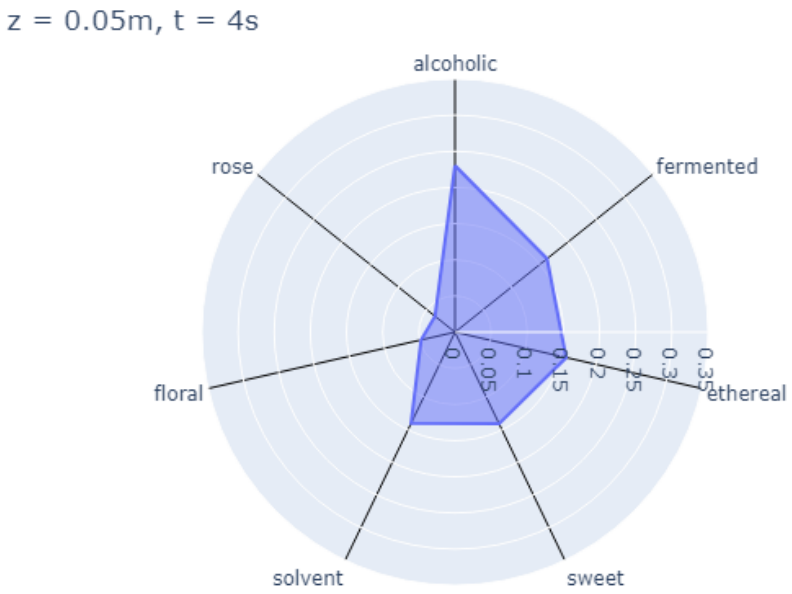

Figure 11: Radar chart depicting the top olfactory families based on their relative frequency of exhibiting the highest intensity at z = 0.05 m, t = 4 s.

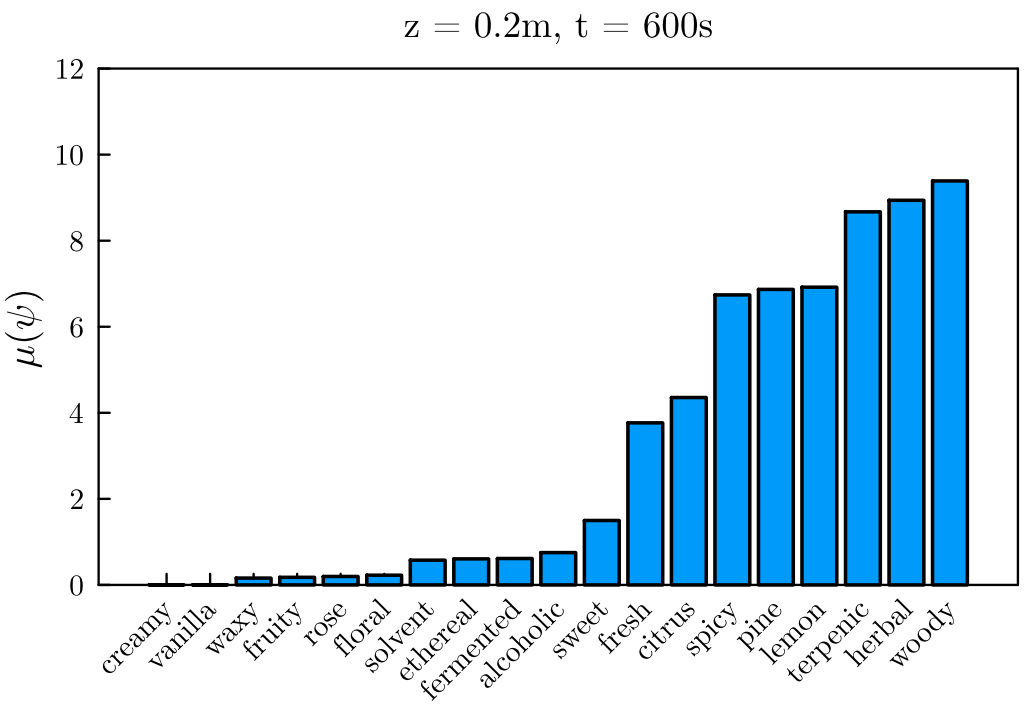

Figure 12: Average intensity distributions for each odor family, presented in ascending order of intensity - z = 0.2 m, t = 600 s.

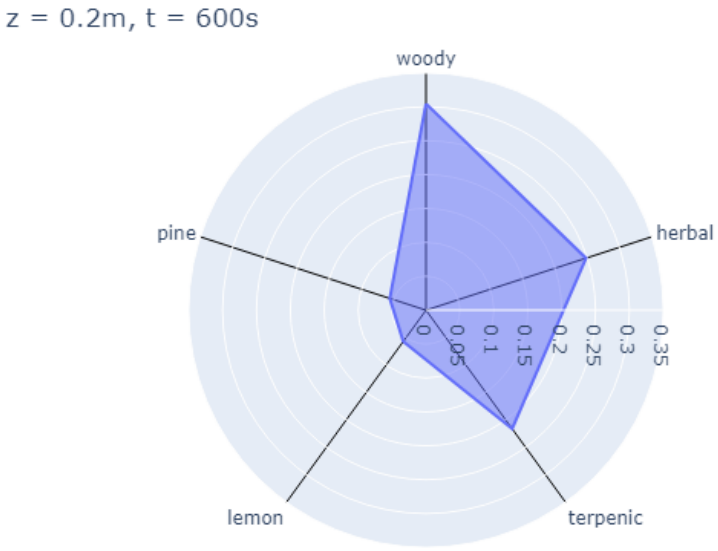

Figure 13: Radar chart depicting the top olfactory families based on their relative frequency of exhibiting the highest intensity at z = 0.2 m, t = 600 s.

4. Conclusions

In conclusion, our research has demonstrated through a quaternary fragrance case study the feasibility of the proposed probabilistic approach for predicting olfactory families of fragranced mixtures. By systematically identifying, quantifying, and incorporating uncertainties in both the perfume diffusion and odor classification models, we have laid the foundation for more robust fragrance design and formulation. It offers a valuable tool for perfumers and fragrance designers, enabling them to assign probabilities to olfactory responses and customize fragrances with a higher likelihood of achieving desired sensory experiences.

One of our unique contributions lies in integrating uncertainty quantification with the odor classification model, leveraging the output probabilities of graph convolutional neural networks to assign weights to odor intensity probability distribution functions and then transforming samples into probabilities by counting dominance. This innovative method enhances the reliability of the predictions and gives a probabilistic estimate of the fragrance's dominant smell.

As a result, our work advances the fragrance science field and contributes to the broader domain of probabilistic modeling in sensory perception. Future research could explore refinements to the methodology, such as incorporating additional sources of uncertainty (either epistemic or aleatoric), extending its applicability to other complex odorant mixtures, and testing the predictive capability against experimental data. Ultimately, the probabilistic approach presented here empowers fragrance designers with a data-driven framework to create perfumes that closely align with desired olfactory profiles, marking a significant step forward in the science of fragrance design.

5. Acknowledgments

This research was supported by the doctoral Grant (reference PRT/BD/152850/2021) and financed by the Portuguese Foundation for Science and Technology (FCT), LA/P/0045/2020 (ALiCE), UIDB/50020/2020 and UIDP/50020/2020 (LSRE-LCM) and with funds from FCT/MCTES (PIDDAC) and State Budgets under MIT Portugal Program.

We want to thank the authors of Clapeyron.jl library, especially Andrés Riedemann, who promptly helped with the thermodynamic part of the model - group assignment and activity coefficient.

Appendix A. Average concentration and quantile ribbons

Figures A.14 and A.15 show the mean concentration over time and the 99% credible intervals (between 5% and 99.5% quantiles) at 0.05 m and 0.5 m from the releasing source.

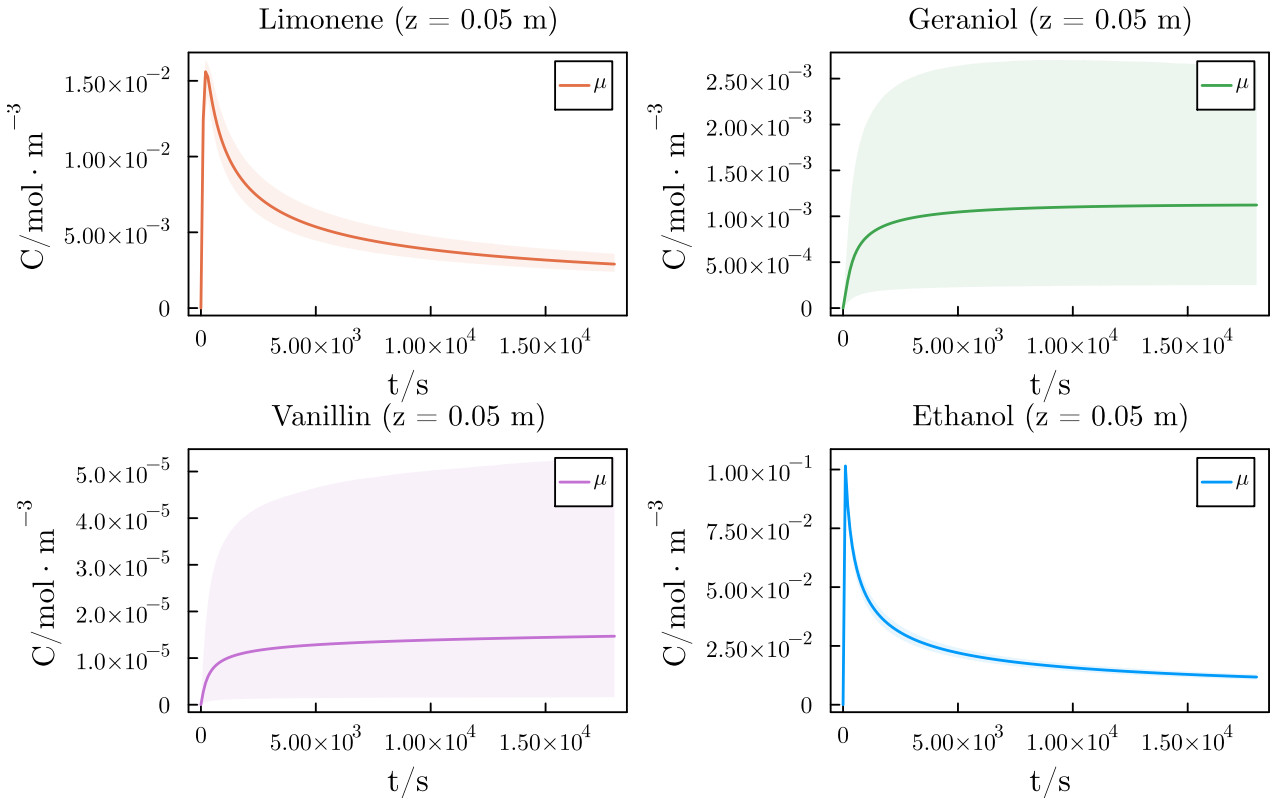

Figure A.14: Mean gas phase concentrations and 99% credible intervals for all components at z = 0.05 m

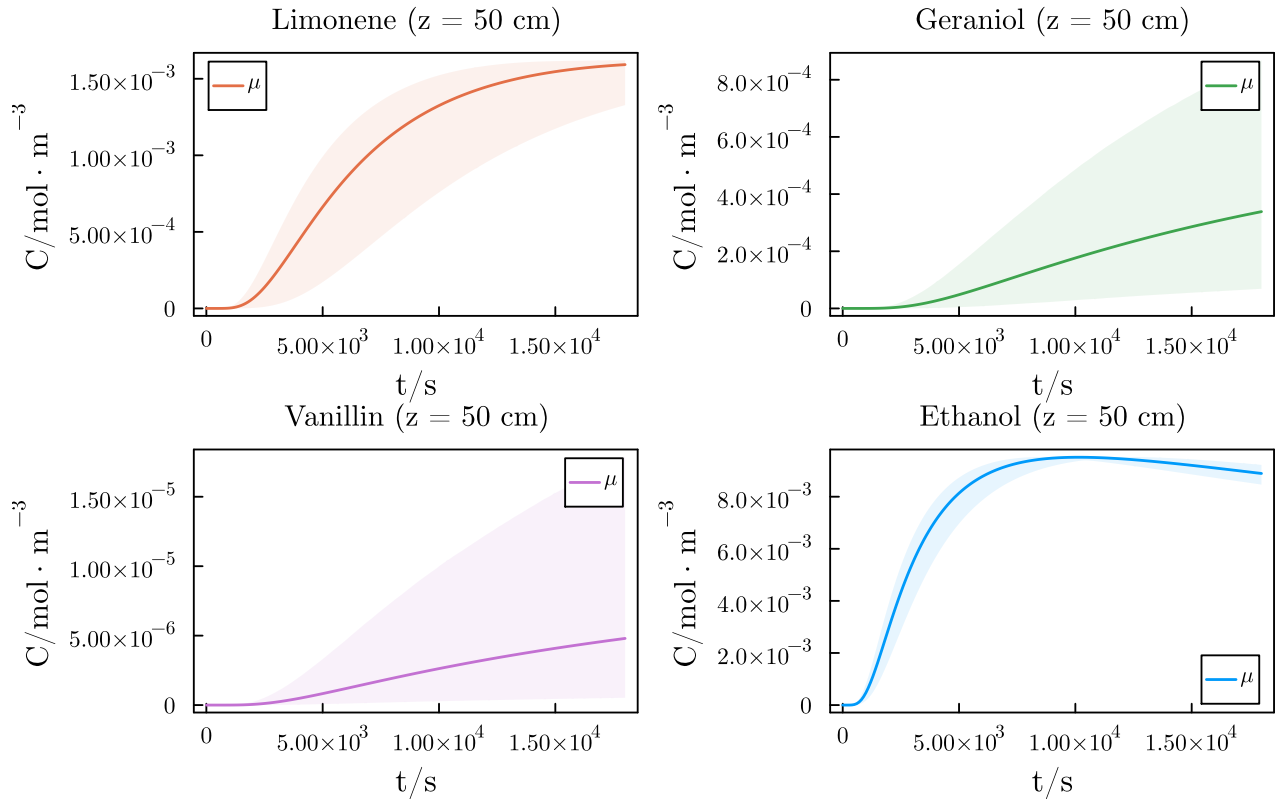

Figure A.15: Mean gas phase concentrations and 99% credible intervals for all components at z = 50 cm

References

Bagge Carlson, F., 2020. Montecarlomeasurements.jl: Nonlinear propagation of arbitrary multivariate distributions by means of method overloading. URL: https://github.com/baggepinnen/MonteCarloMeasurements.jl, arXiv:2001.07625.

Barsainyan, Aryan Amit;Schmuker, M., 2023. Open principal odor map. https://github.com/ARY2260/openpom.

Besançon, M., Papamarkou, T., Anthoff, D., Arslan, A., Byrne, S., Lin, D., Pearson, J., 2021. Distributions.jl: Definition and modeling of probability distributions in the juliastats ecosystem. Journal of Statistical Software 98, 1–30. URL: https://www.jstatsoft.org/v098/i16, doi:10.18637/jss.v098.i16.

Bezanson, J., Karpinski, S., Shah, V.B., Edelman, A., 2012. Julia: A fast dynamic language for technical computing. arXiv preprint arXiv:1209.5145 .

Butler, H., 2013. Poucher's perfumes, cosmetics and soaps. Springer Science & Business Media.

Cain, W.S., Schiet, F.T., Olsson, M.J., de Wijk, R.A., 1995. Comparison of models of odor interaction. Chemical senses 20, 625–637.

Calkin, R.R., Jellinek, J.S., 1994. Perfumery: practice and principles. John Wiley & Sons.

Chambers, E., Wolf, M., 1996. Sensory testing methods. URL: https://books.google.no/books?id=c5I8vwEACAAJ.

Chapman, S., Cowling, T., 1990. The Mathematical Theory of Non-uniform Gases: An Account of the Kinetic Theory of Viscosity, Thermal Conduction and Diffusion in Gases. Cambridge Mathematical Library, Cambridge University Press. URL: https://books.google.no/books?id=Cbp5JP2OTrwC.

Cussler, E., Wagner, A., Marchal-Heussler, L., 2010. Designing chemical products requires more knowledge of perception. AIChE Journal 56, 283–288.

Fuller, E.N., Schettler, P.D., Giddings, J.C., 1966. New method for prediction of binary gas-phase diffusion coefficients. Industrial & Engineering Chemistry 58, 18–27. URL: https://doi.org/10.1021/ie50677a007, doi:10.1021/ie50677a007.

van Gemert, L., 2011. Odour thresholds: compilations of odour threshold values in air, water and other media. URL: https://books.google.no/books?id=ZfC6twAACAAJ.

Gilbert, A., 2008. What the nose knows: The science of scent in everyday life.

GmbH, D., 2023. Vapor pressure of ethanol. URL: www.ddbst.com.

Gmehling, J., 2003. Potential of group contribution methods for the prediction of phase equilibria and excess properties of complex mixtures. Pure and applied chemistry 75, 875–888.

Gmehling, J., Wittig, R., Lohmann, J., Joh, R., 2002. A modified unifac (dortmund) model. 4. revision and extension. Industrial & Engineering Chemistry Research 41, 1678–1688. URL: https://doi.org/10.1021/ie0108043, doi:10.1021/ie0108043.

Hardin, R., Sloane, N., 1993. A new approach to the construction of optimal designs. Journal of Statistical Planning and Inference 37, 339–369. URL: https://www.sciencedirect.com/science/article/pii/037837589390112J, doi:https://doi.org/10.1016/0378-3758(93)90112-J.

Keller, A., Gerkin, R.C., Guan, Y., Dhurandhar, A., Turu, G., Szalai, B., Mainland, J.D., Ihara, Y., Yu, C.W., Wolfinger, R., Vens, C., leander schietgat, Grave, K.D., Norel, R., Consortium, D.O.P., Stolovitzky, G., Cecchi, G.A., Vosshall, L.B., pablo meyer, 2017. Predicting human olfactory perception from chemical features of odor molecules. Science 355, 820–826. URL: https://www.science.org/doi/abs/10.1126/science.aal2014, doi:10.1126/science.aal2014, arXiv:https://www.science.org/doi/pdf/10.1126/science.aal2014.

Keller, A., Vosshall, L.B., 2016. Olfactory perception of chemically diverse molecules. BMC Neuroscience , 1–17doi:10.1186/s12868-016-0287-2.

Laffort, P., Dravnieks, A., 1982. Several models of suprathreshold quantitative olfactory interaction in humans applied to binary, ternary and quaternary mixtures. Chemical Senses 7, 153–174.

Lee, B.K., Mayhew, E.J., Sanchez-Lengeling, B., Wei, J.N., Qian, W.W., Little, K.A., Andres, M., Nguyen, B.B., Moloy, T., Yasonik, J., Parker, J.K., Gerkin, R.C., Mainland, J.D., Wiltschko, A.B., 2023. A principal odor map unifies diverse tasks in olfactory perception. Science 381, 999–1006. URL: https://www.science.org/doi/abs/10.1126/science.ade4401, doi:10.1126/science.ade4401, arXiv:https://www.science.org/doi/pdf/10.1126/science.ade4401.

Lin, D., White, J.M., Byrne, S., Bates, D., Noack, A., Pearson, J., Arslan, A., Squire, K., Anthoff, D., Papamarkou, T., Besançon, M., Drugowitsch, J., Schauer, M., other contributors, 2019. JuliaStats/Distributions.jl: a Julia package for probability distributions and associated functions. URL: https://doi.org/10.5281/zenodo.2647458, doi:10.5281/zenodo.2647458.

Massey, F.J., 1951. The kolmogorov-smirnov test for goodness of fit. Journal of the American Statistical Association 46, 68–78. URL: http://www.jstor.org/stable/2280095.

Mata, V.G., Gomes, P.B., Rodrigues, A.E., 2005. Perfurmery ternary diagrams (ptd): A new concept applied to the optimization of perfume compositions. Flavour and Fragrance Journal 20, 465–471. doi:10.1002/ffj.1590.

Olsson, M.J., 1998. An integrated model of intensity and quality of odor mixtures. Annals of the New York Academy of Sciences 855, 837–840.

Poling, B.E., Prausnitz, J.M., O'connell, J.P., 2001. Properties of gases and liquids. McGraw-Hill Education.

Rackauckas, C., Nie, Q., 2017. DifferentialEquations.jl–a performant and feature-rich ecosystem for solving differential equations in Julia. Journal of Open Research Software 5.

Rodrigues, A.E., Nogueira, I., Faria, R.P.V., 2021. Perfume and flavor engineering: A chemi-

cal engineering perspective. Molecules 26. URL: https://www.mdpi.com/1420-3049/26/11/3095, doi:10.3390/molecules26113095.

Sanchez-Lengeling, B., Wei, J.N., Lee, B.K., Gerkin, R.C., Aspuru-Guzik, A., Wiltschko, A.B., 2019. Machine learning for scent: Learning generalizable perceptual representations of small molecules. arXiv:1910.10685.

Santana, V.V., Martins, M.A., Loureiro, J.M., Ribeiro, A.M., Rodrigues, A.E., Nogueira, I.B., 2021. Optimal fragrances formulation using a deep learning neural network architecture: A novel systematic approach. Computers and Chemical Engineering 150, 107344. doi:10.1016/j.compchemeng.2021.107344.

Sobol', I., 1967. On the distribution of points in a cube and the approximate evaluation of integrals. USSR Computational Mathematics and Mathematical Physics 7, 86–112. URL: https://www.sciencedirect.com/science/article/pii/0041555367901449, doi:https://doi.org/10.1016/0041-5553(67)90144-9.

Stephenson, R.M., Malanowski, S., 1987. Handbook of the Thermodynamics of Organic Compounds. Springer Netherlands. doi:10.1007/978-94-009-3173-2.

Teixeira, M., Rodríguez, O., Gomes, P., Mata, V., Rodrigues, A.E., 2013a. Perfume engineering: Design, performance & classification. doi:10.1016/B978-0-08-099399-7.00006-7.

Teixeira, M.A., Barrault, L., Rodríguez, O., Carvalho, C.C., Rodrigues, A.E., 2014. Perfumery radar 2.0: A step toward fragrance design and classification. Industrial & Engineering Chemistry Research 53, 8890–8912. URL: https://doi.org/10.1021/ie403968w, doi:10.1021/ie403968w, arXiv:https://doi.org/10.1021/ie403968w.

Teixeira, M.A., Rodríguez, O., Rodrigues, A.E., 2010. The perception of fragrance mixtures: A comparison of odor intensity models. Aiche Journal 56, 1090–1106. URL: https://api.semanticscholar.org/CorpusID:97192105.

Teixeira, M.A., Rodríguez, O., Mata, V.G., Rodrigues, A.E., 2009. The diffusion of perfume mixtures and the odor performance. Chemical Engineering Science 64, 2570–2589. URL: https://www.sciencedirect.com/science/article/pii/S0009250909000700, doi:https://doi.org/10.1016/j.ces.2009.01.064.

Teixeira, M.A., Rodríguez, O., Mota, F.L., Macedo, E.A., Rodrigues, A.E., 2011. Evaluation of group-contribution methods to predict vle and odor intensity of fragrances. Industrial & Engineering Chemistry Research 50, 9390–9402. URL: https://doi.org/10.1021/ie200290r, doi:10.1021/ie200290r, arXiv:https://doi.org/10.1021/ie200290r.

Teixeira, M.A., Rodríguez, O., Rodrigues, A.E., 2013b. Diffusion and performance of fragranced products: Prediction and validation. AIChE Journal doi:10.1002/aic.14106.

Teixeira, M.A.A., 2011. Perfume performance and classification: Perfumery quaternary-quinary diagram

(pq2d®) and perfumery radar. Futures , 725–752doi:10.1002/fut.

Ulas, S., Diwekar, U.M., 2004. Thermodynamic uncertainties in batch processing and optimal control. Computers & Chemical Engineering 28, 2245–2258. URL: https://www.sciencedirect.com/science/article/pii/S0098135404001061, doi:https://doi.org/10.1016/j.compchemeng.2004.04.001.

Walker, P.J., Yew, H.W., Riedemann, A., 2022. Clapeyron.jl: An extensible, open-source fluid thermodynamics toolkit. Industrial & Engineering Chemistry Research 61, 7130–7153. URL: https://doi.org/10.1021/acs.iecr.2c00326, doi:10.1021/acs.iecr.2c00326.

Zhang, X., Zhou, T., Ng, K.M., 2020. Optimization-based cosmetic formulation: Integration of mechanistic model, surrogate model, and heuristics. AIChE Journal doi:10.1002/aic.17064.